THE ASTROPHYSICAL JOURNAL, 524:92–97, 1999 October 10
© 1999. The American Astronomical Society. All rights reserved. Printed in U.S.A.

A *ROSAT* DEEP SURVEY OF FOUR SMALL GAMMA-RAY BURST ERROR BOXES

K. HURLEY AND P. LI
University of California at Berkeley, Space Sciences Laboratory, CA 94720-7450; khurley@sunspot.ssl.berkeley.edu
M. BOER
CESR, B.P. 4346, 31029 Toulouse Cedex, France
T. CLINE
Goddard Space Flight Center, Code 661, Greenbelt, MD 20771
G. J. FISHMAN AND C. MEEGAN
Marshall Space Flight Center ES 62, Huntsville, AL 35812
C. KOUVELIOTOU
Universities Space Research Association, Marshall Space Flight Center ES-84, Huntsville, AL 35812
J. GREINER
MPE, D-85740 Garching, Germany
J. LAROS
University of Arizona, Department of Planetary Sciences, Tucson, AZ 85721
C. LUGINBUHL AND F. VRBA
US Naval Observatory, Flagstaff Station, P.O. Box 1149, Flagstaff, AZ 86002-1149
T. MURAKAMI
ISAS, 3-1, Yoshinodai, Sagamihara, Kanagawa 229, Japan
H. PEDERSEN
Copenhagen University Observatory, Oster Voldgade 3, DK 1350, Copenhagen, Denmark
AND
J. VAN PARADIJS[1]
University of Alabama in Huntsville, Huntsville, AL 35899
Received 1999 March 24; accepted 1999 June 1

ABSTRACT

We have used the *ROSAT* High Resolution Imager to search for quiescent X-ray counterparts to four gamma-ray bursts (GRBs) which were localized to small (≤ 10 arcmin^2) error boxes with the Interplanetary Network. The observations took place years after the bursts, and the effective exposure times for each target varied from ~ 16 to 23 ks. We have not found any X-ray sources inside any of the error boxes. The 0.1–2.4 keV 3 σ flux upper limits range from around 5×10^{-14} to 6×10^{-13} ergs cm^{-2} s^{-1} depending on the burst and the assumed shape of the quiescent spectrum. We consider four types of X-ray–emitting galaxies (normal, active galactic nucleus, faint, and star forming) and use the flux upper limits to constrain their redshifts. We then use the GRB fluences to constrain the total energies of the bursts.

Subject headings: galaxies: distances and redshifts — gamma rays: bursts — X-rays: galaxies

1. INTRODUCTION

The cosmic gamma-ray burst distance scale was a mystery until the recent discovery of X-ray afterglows by *BeppoSAX* and of optical and radio afterglows from some of these gamma-ray bursts (GRBs). These observations have made it possible to estimate the GRB distance scale from the redshift of the optical counterparts. Four spectroscopic redshift measurements have now been obtained: $z = 0.835$ for GRB 970508 (Metzger et al. 1997; Bloom et al. 1998a), $z = 3.4$ for GRB 971214 (Kulkarni et al. 1998), $z = 0.966$ for GRB 980703 (Djorgovski et al. 1998), and $z = 1.6$ for GRB 990123 (Hjorth et al. 1999). The nature of the host galaxies in these cases is not clear, although in one case the host appears to be in an active star formation phase (Djorgovski et al. 1998). While it is now generally accepted that GRBs are at cosmological distances, the picture is clouded by the apparent association of one burst, GRB 980425, with a nearby ($z = 0.008$) supernova, SN1998bw, in a barred spiral galaxy, ESO 184-G82 (Galama et al. 1998). Although there is evidence that GRBs are not *generally* associated with supernovae (Kippen et al. 1998), it has been argued that perhaps 1% could be (Bloom et al. 1998b). Similarly, it has been argued that GRBs are associated with Abell clusters (Kolatt & Piran 1996; Struble & Rood 1997) and radio-quiet quasars (Schartel, Andernach, & Greiner 1997). While the latter two associations are probably not valid (Hurley et al. 1999), all these claimed associations serve to demonstrate that the nature of GRB host galaxies is not yet well understood. Indeed, the evidence is not inconsistent with the suggestion that short gamma-ray bursts have a different origin from long ones (Pizzichini 1995; Belli 1997; Tavani 1998; but see also Kouveliotou et al. 1996 and Pendleton 1997). Counterpart observations in the X-ray, optical, and radio ranges at various times after the bursts will continue to be valuable for unraveling these issues.

[1] Astronomical Institute "Anton Pannekoek," University of Amsterdam, Kruislaan 403, 1098SJ Amsterdam, The Netherlands.

In this paper we present *ROSAT* soft X-ray observations of four GRB error boxes. The objective of this study was to detect quiescent X-ray counterparts to GRB sources. Accordingly, the observations took place years after the bursts. (At the sensitivity levels of this survey, the fading X-ray counterparts to these bursts would have been undetectable days to a week after the bursts.) The GRB locations were obtained with the Interplanetary Network (IPN), composed of *Ulysses*, BATSE aboard the *Compton Gamma Ray Observatory*, and either the *Pioneer Venus Orbiter* or *Mars Observer* spacecraft at the times of these bursts. The error boxes have been published by Laros et al. (1997, 1998), and the properties of the bursts have appeared in Meegan et al. (1996). The bursts were selected for study based on three criteria: their high Galactic latitude and/or the error box area (from which the probability of detecting a random source within the error box can be estimated) and the maximum error box dimension (so that the error box could be covered in a single *ROSAT* High Resolution Imager [HRI] pointing).

Previous soft X-ray surveys of GRB error boxes have appeared. These were based on *Einstein* and *EXOSAT* observations (Pizzichini et al. 1986; Boer et al. 1988). With one exception, these observations resulted in upper limits which were approximately 1 to several orders of magnitude greater than the results of the present survey. The exception is the case of GRB 781119 (see, e.g., Hurley et al. 1996 and references therein), where a persistent X-ray source was detected. However, its relation to the GRB is unclear.

2. *ROSAT* RESULTS

Table 1 gives the properties of the bursts and the results of the observations. The BATSE trigger number (Meegan et al. 1996) appears in the first row, and the *ROSAT* sequence number in the second. The Galactic latitude, longitude, and error box area are given in the next three rows. The sixth row gives the approximate 25–150 keV fluence, estimated from the *Ulysses* observations; all of the bursts are rather bright (or they would not have been detected by the relatively small instruments of the IPN) and thus, presumably, relatively nearby. In principle, the source distance may be estimated from the fluence; in practice, this estimate depends strongly on the assumed cosmological constants, assumptions about source evolution, and beaming of the emission. We have included a range of redshift estimates in the seventh row based on standard candle luminosities of 10^{51} and 10^{53} ergs s^{-1} and on an $\Omega = 1$, $\Lambda = 0$ universe (see § 3.1). The following row gives the total effective observation time by *ROSAT*. All observations took place with the HRI, in the 0.07–2.4 keV energy band. The ninth row gives the elapsed time between the burst and the observation. In this particular study no attempt was made to minimize this time interval, as the objective was the study of long-lived, quiescent counterparts. The 10th row indicates whether a source was observed within the IPN error box. The 11th row gives the number of sources in the HRI field of view. The 12th row gives the a posteriori probability of finding a source in the error box by chance. It is calculated simply as the number of sources times the ratio of the error box area to the area of the HRI field of view. (The number of sources is consistent with the number of background sources expected at these sensitivity levels.) The 13th row gives the hydrogen column density along the line of sight. The last three rows give the upper limits to the 0.1–2.4 keV flux of any source in the error box assuming thermal bremsstrahlung, blackbody, and power-law spectra, corrected for the foreground column density. Depending on the column density and the assumed spectral form, different spectral parameters may result in upper limits which differ by a factor of 2–3.

The *ROSAT* data were analyzed using the standard data analysis tools and data cuts. In these observations there is presently a spacecraft pointing error (the "boresight error") that is generally less than 10″. As this is much smaller than the error box sizes, and since the boresight-corrected data were not all available at the time of this writing, we have ignored this. The data selection criteria are given by Gruber et al. (1996). The IRAF/PROS sliding window source detection technique and software were used to identify the sources in each image (we used a signal-to-noise ratio of 3 for our source detection criterion). To obtain the 3 σ upper limits, the source counts and background counts were taken from the same image. The source box center was at the GRB error box center. The background box was centered at a location where it excluded the GRB error box and any sources in the field. The box size was initially chosen to be

TABLE 1

GRB PROPERTIES AND *ROSAT* RESULTS

Parameter	GRB 910522	GRB 920325	GRB 920406	GRB 930706
BATSE number	219	1519	1541	2431
ROSAT observation number	US400882H	US400881H	US400879H	US400880H
b (deg)	−2	−44	−26	−7
l (deg)	272	92	339	14
Error box size (arcmin^2)	9.3	4.8	0.44	4.0
Fluence (ergs cm^{-2})	3×10^{-5}	5×10^{-6}	1.4×10^{-4}	2×10^{-5}
Estimated redshift z	0.1–0.6	0.2–1.1	0.05–0.4	0.1–0.7
Observation time (s)	19,748	16,008	21,018	22,869
Time since GRB (yr)	6.50	5.17	5.50	4.25
Source in error box?	No	No	No	No
Total number of sources in 40′ field of view	5	6	5	5
A posteriori chance detection probability	0.037	0.023	0.0018	0.016
N_H (cm^{-2})	1.35×10^{22}	4.32×10^{20}	5.34×10^{20}	1.92×10^{21}
3 σ flux upper limit (bremsstrahlung) (ergs cm^{-2} s^{-1})	6.2×10^{-13}	6.4×10^{-14}	5.2×10^{-14}	7.5×10^{-14}
3 σ flux upper limit (blackbody) (ergs cm^{-2} s^{-1})	2.8×10^{-13}	6.8×10^{-14}	5.3×10^{-14}	6.2×10^{-14}
3 σ flux upper limit (power law) (ergs cm^{-2} s^{-1})	3.2×10^{-13}	6.0×10^{-14}	7.0×10^{-14}	7.9×10^{-14}

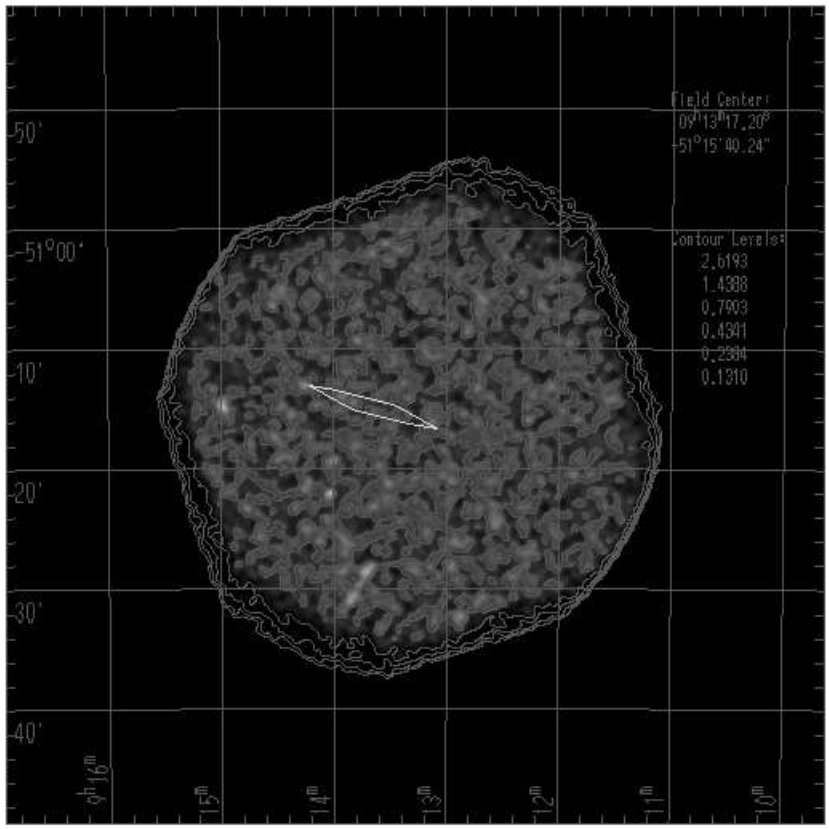

FIG. 1.—*ROSAT* HRI image of the GRB 910522 field with the approximate position of the IPN error box

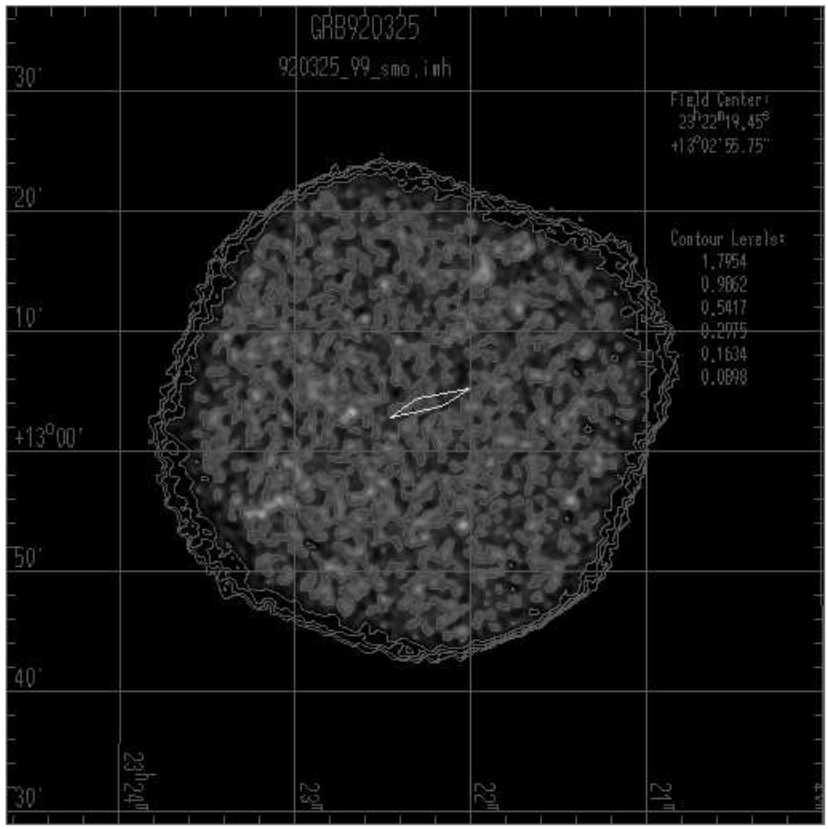

FIG. 2.—*ROSAT* HRI image of the GRB 920325 field with the approximate position of the IPN error box

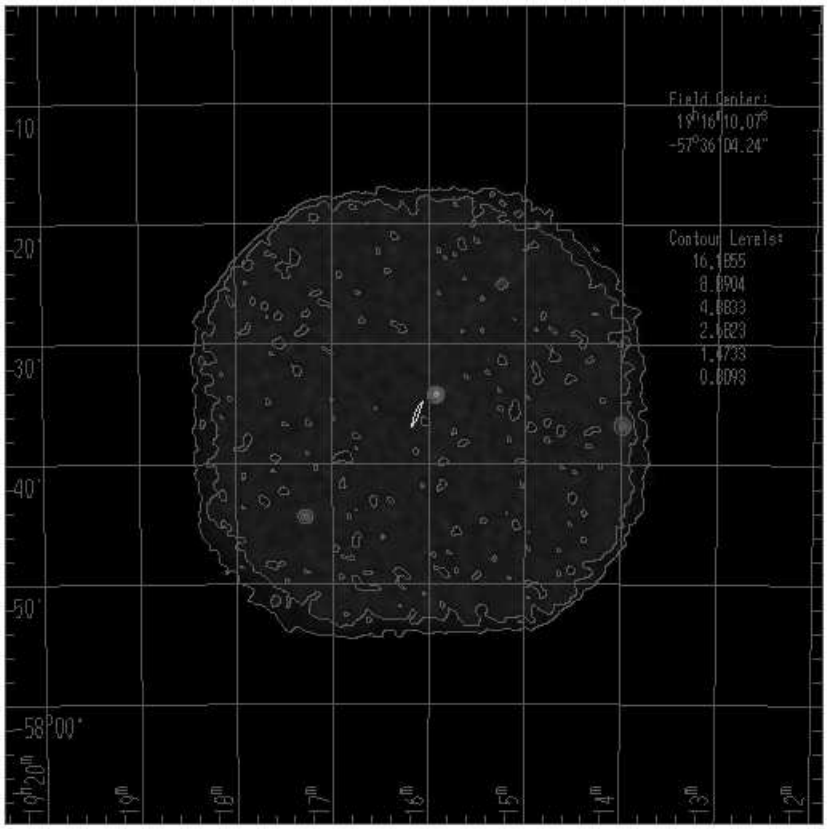

FIG. 3.—*ROSAT* HRI image of the GRB 920406 field with the approximate position of the IPN error box

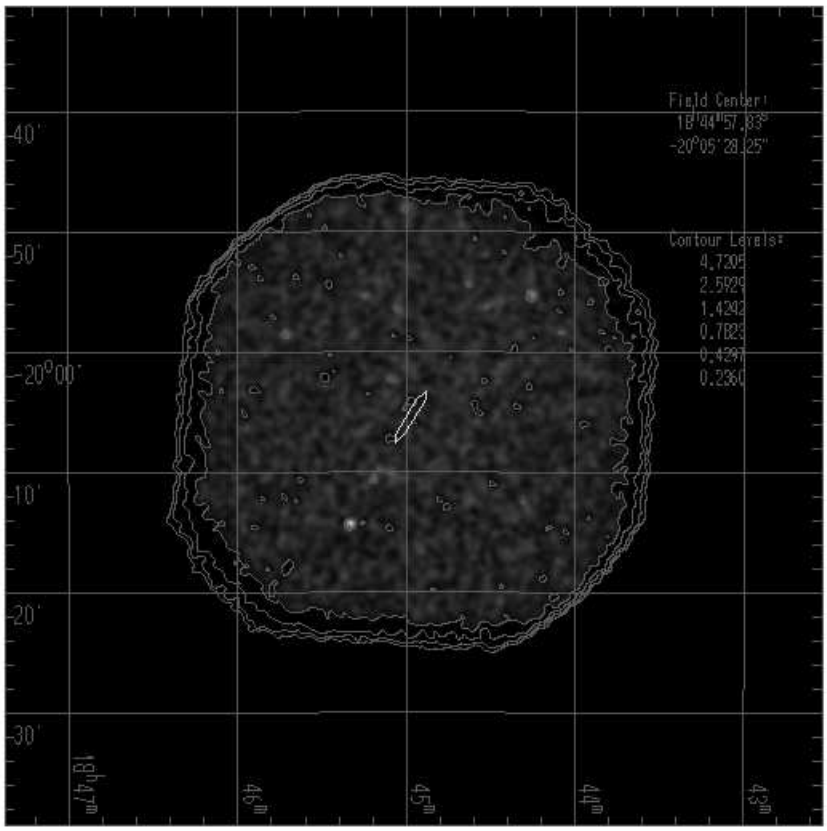

FIG. 4.—*ROSAT* HRI image of the GRB 930706 field with the approximate position of the IPN error box

$32'' \times 32''$. The *ROSAT* HRI point-spread function is such that this box contains 90% of the energy of a point source. The box size was the same for both source and background estimates. The column density for each GRB error box was obtained from the HEASARC W3nH program, based on Dickey & Lockman (1990).[2] The large column density for GRB 910522, which lies only 2° from the Galactic plane, explains the larger flux upper limits for this source. The HRI images with the GRB error boxes are shown in Figures 1–4.

The 3 σ count upper limit was then converted to flux for three assumed spectral models since the HRI does not give spectral information. For the thermal bremsstrahlung and blackbody models, a temperature $kT = 1$ keV was assumed. For the power-law model, the assumed photon spectral index was -1. With the kT or spectral index and the line-of-sight column density, we used PIMMS (Portable Interactive Multi-Mission Simulator, available through the HEASARC[3]) to convert the 3 σ count rate upper limit to a 0.1–2.4 keV 3 σ flux upper limit.

3. CONSTRAINTS ON GRB HOST GALAXIES

All of the bursts in Table 1 would probably be classified as "long." One possible exception is GRB 920325. No duration is given for this event in the BATSE Catalog (Meegan et al. 1996). The burst consists of a short (<1 s) initial spike but is followed by low-level emission for several seconds. The next shortest event, GRB 930706, has a T_{90} duration of 2.7 s, placing it between the "short" and "long" peaks of the duration distribution, but on the shoulder of the "long" bursts. We therefore assume that these GRBs are similar to the four for which redshifts have been measured and that they originated in or very close to galaxies. The X-ray flux upper limits may therefore be used to derive lower limits to the distances of the hosts. From this, in turn, we may obtain lower limits on the GRB energy.

3.1. *Galaxy Types and Distance Scale*

Galaxies display a wide range of X-ray luminosities. The X-rays from normal galaxies come from individual sources such as binaries and supernova remnants, as well as from a hot phase of the interstellar medium, heated by supernovae; their X-ray luminosities range from $L_X = 10^{38}$ to 10^{42} ergs s^{-1} (Fabbiano 1989). The X-ray emission from AGNs is thought to be powered by supermassive black holes; AGN X-ray luminosities range from $L_X = 10^{42}$ to 10^{46} ergs s^{-1} (Maccacaro et al. 1991). Perhaps more relevant to the host galaxies of gamma-ray bursts, studies of faint galaxies ($B \leq 23$) at redshifts $0.1 < z < 0.5$ show that they have X-ray luminosities $L_X = 10^{41.5}$–10^{43} ergs s^{-1} (Roche et al. 1995). These rather large X-ray luminosities are apparently not due to a Malmquist bias, since their L_X/L_B ratios are an order of magnitude larger than most local galaxies. Finally, studies of star-forming galaxies, whose X-ray emission may be due to massive X-ray binaries, indicate that their luminosities are $L_X = 10^{39.5}$–$10^{41.5}$ ergs s^{-1} (Griffiths & Padovani 1990).

In an $\Omega = 1$, $\Lambda = 0$ universe, the quiescent X-ray luminosity L_0, the luminosity distance d_L, and the observed X-ray flux F_X are related through

$$F_X = \frac{L_0(1+z)^{-\alpha}}{4\pi d_L^2}, \quad (1)$$

where z is the redshift and the photon spectrum of the quiescent X-ray source is assumed to be a power law with photon index α. The luminosity distance is given by

$$d_L = \frac{2c[1+z-(1+z)^{1/2}]}{H_0}, \quad (2)$$

where c is the speed of light and H_0 is the Hubble constant. Equations (1) and (2) may be used to derive a lower limit to the redshift of each of the four bursts, assuming a specific galaxy type. From this the total gamma-ray energy in the burst may be calculated:

$$E_\gamma = 4\pi f d_L^2 (1+z)^n, \quad (3)$$

where f is the burst fluence and the spectral shape of the burst is assumed to be a power law with photon index n. In Table 2 distance lower limits to each burst are given for the four galaxy types for the lower and upper limit to the X-ray luminosity. A lower limit to the total isotropic burst energy is also calculated. We have assumed that the X-ray spectrum is given by a power law with $\alpha = -1$ and that the GRB spectrum is described by a power law with $n = -2$, and we have taken $H_0 = 65$ km s^{-1} Mpc^{-1}. These numbers are not very sensitive to the choice of Ω; for example, using the approximation of Pen (1999), if we take $\Omega = 0.3$, the luminosity distance changes by only 2% for $z = 0.04$ and by 10% for $z = 0.2$.

4. DISCUSSION

Numerous multiwavelength follow-up observations have been performed on the four GRB error boxes in this study, including Barthelmy, Palmer, & Schaefer (1994; Schmidt telescope observations); Luginbuhl et al. (1995; *UBVI* observations at the US Naval Observatory); Hurley et al. (1995; extreme ultraviolet observation with the *EUVE* spacecraft); Luginbuhl et al. (1996; optical observations at

[2] http://heasarc.gsfc.nasa.gov/docs/frames/hhp_sw.html.
[3] http://heasarc.gsfc.nasa.gov/Tools/w3pimms.html.

TABLE 2

LOWER LIMITS TO GRB HOST GALAXY REDSHIFTS AND TOTAL GRB ENERGIES FOR FOUR TYPES OF GALAXIES

Parameter	GRB 910522	GRB 920325	GRB 920406	GRB 930706
z (normal)	>0.0004–0.04	>0.0008–0.08	>0.0008–0.07	> 0.0007–0.07
E_γ (normal) (ergs)	$>1 \times 10^{46}$–1×10^{50}	$>8 \times 10^{45}$–9×10^{49}	$>2 \times 10^{47}$–2×10^{51}	$>3 \times 10^{46}$–3×10^{50}
z (AGN)	>0.04–1.8	>0.08–3.1	>0.07–3.0	>0.07–2.8
E_γ (AGN) (ergs)	$>1 \times 10^{50}$–3×10^{54}	$>9 \times 10^{49}$–3×10^{54}	$>2 \times 10^{51}$–8×10^{55}	$>3 \times 10^{50}$–1×10^{55}
z (faint)	>0.02–0.1	>0.04–0.2	>0.04–0.2	>0.04–0.2
E_γ (faint) (ergs)	$>3 \times 10^{49}$–1×10^{51}	$>3 \times 10^{49}$–1×10^{51}	$>7 \times 10^{50}$–2×10^{52}	$>8 \times 10^{49}$–3×10^{51}
z (star forming)	>0.002–0.02	>0.005–0.04	>0.004–0.04	>0.004–0.04
E_γ (star forming) (ergs)	$>3 \times 10^{47}$–3×10^{49}	$>3 \times 10^{47}$–3×10^{49}	$>6 \times 10^{48}$–7×10^{50}	$>8 \times 10^{47}$–8×10^{49}

US Naval Observatory and Cerro Tololo Inter-American Observatory); Schaefer et al. (1997; *Hubble Space Telescope* observations in the *B*, *U*, and UV bands); Larson & McLean (1997; near-infrared observations); Schaefer et al. (1998; ground-based optical observations); and Vrba et al. (1998; *UBVI* observations at the USNO). Although no counterparts were identified in any of these observations, the sensitivities in many cases would have been insufficient to detect the faint galaxies which have been found in later studies by searching at the precisely known positions of the brighter optical transients. Except for GRB 980425, where the association of the galaxy with the GRB is still debatable, the nature of the host galaxies found so far is uncertain. If they are faint or star-forming galaxies at redshifts ~ 1, and if the four bursts in this study have similar hosts, then it is clear from Table 2 why no quiescent X-ray sources were detected; the sensitivity would have allowed the detection of such objects only out to redshifts of ~ 0.2 at best.

Assuming a sensitivity of 3×10^{-15} ergs cm^{-2} s^{-1} for a deep *Chandra X-Ray Observatory* or *XMM* observation, the quiescent X-ray emission from normal, faint, or star-forming galaxies could be detected out to redshifts of 0.3, 0.8, and 0.2, respectively. It is therefore possible that the quiescent X-ray counterparts to the closer bursts could be detected. It is also possible that the short GRBs originate at smaller distances (as their number-intensity relation suggests), making the X-ray detection of their host galaxies feasible.

The work at UC Berkeley was supported by grant NAG5-1727 from the US *ROSAT* guest investigator program and has made use of data obtained from the High Energy Astrophysics Science Archive Research Center (HEASARC), provided by NASA's Goddard Space Flight Center.

REFERENCES

Barthelmy, S., Palmer, D., & Schaefer, B. 1994, in AIP Conf. Proc. 307, Gamma-Ray Bursts, Second Workshop, ed. G. Fishman, J. Brainerd, & K. Hurley (New York: AIP), 392
Belli, B. 1997, ApJ, 479, L31
Bloom, J., Djorgovski, S., Kulkarni, S., & Frail, D. 1998a, ApJ, 507, L25
Bloom, J., Kulkarni, S., Harrision, F., Prince, T., Phinney, E., & Frail, D. 1998b, ApJ, 506, L105
Boer, M., et al. 1988, A&A, 202, 117
Dickey, J., & Lockman, F. 1990, ARA&A, 28, 215
Djorgovski, S., Kulkarni, S., Bloom, J., Goodrich, R., Frail, D., Piro, L., & Palazzi, E. 1998, ApJ, 508, L17
Fabbiano, G. 1989, ARA&A, 27, 87
Galama, T., et al. 1998, Nature, 395, 670
Griffiths, R., & Padovani, P. 1990, ApJ, 360, 483
Gruber, R., et al. 1996, in The *ROSAT* User's Handbook, ed. U. Briel (Garching: MPI)
Hjorth, J., et al. 1999, GCN Circ. 219, http://gcn.gsfc.nasa.gov/gcn/gcn3/219.gcn3
Hurley, K., Hartmann, D., Kouveliotou, C., Kippen, R. M., Laros, J., Cline, T., & Boer, M. 1999, ApJ, 515, 497
Hurley, K., Li, P., Laros, J., Fishman, G., Kouveliotou, C., & Meegan, C. 1995, ApJ, 445, 348
Hurley, K., et al. 1996, ApJ, 469, L105
Kippen, R., et al. 1998, ApJ, 506, L27,
Kolatt, T., & Piran, T. 1996, ApJ, 467, L41
Kouveliotou, C. 1996, in AIP Conf. Proc. 384, Proc. Third Huntsville Workshop on Gamma-Ray Bursts, ed. C. Kouveliotou, M. S. Briggs, & G. J. Fishman (New York: AIP), 42
Kulkarni, S., et al. 1998, Nature, 393, 35
Laros, J., et al. 1997, ApJS, 110, 157
———. 1998, ApJS, 118, 391
Larson, S., & McLean, I. 1997, ApJ, 491, 93
Luginbuhl, C., et al. 1995, Ap&SS, 231(1/2), 289
———. 1996, in AIP Conf. Proc. 384, Proc. Third Huntsville Workshop on Gamma-Ray Bursts, ed. C. Kouveliotou, M. S. Briggs, & G. J. Fishman (New York: AIP), 676
Maccacaro, T., Della Ceca, R., Gioia, M., Morris, S., Stocke, J., & Wolter, A. 1991, ApJ, 374, 117
Meegan, C., et al. 1996, ApJS, 106, 45
Metzger, M., et al. 1997, Nature, 387, 878
Pen, U. 1999, ApJS, 120, 49
Pendleton, G. 1997, ApJ, 489, 175
Pizzichini, G. 1995, in Proc. 24th Int. Cosmic-Ray Conf. (Rome) OG2.1.8, 81
Pizzichini, G., et al. 1986, ApJ, 301, 641
Roche, N., Shanks, T., Georgantopoulos, I., Stewart, G., Boyle, B., & Griffiths, R. 1995, MNRAS, 273, L15
Schaefer, B., Cline, T., Hurley, K., & Laros, J. 1997, ApJ, 489, 697
———. 1998, ApJS, 118, 353
Schartel, N., Andernach, H., & Greiner, J. 1997, A&A, 323, 659
Struble, M., & Rood, H. 1997, ApJ, 490, 109
Tavani, M. 1998, ApJ, 497, L21
Vrba, F., et al. 1998, in AIP Conf. Proc. 428, Gamma-Ray Bursts, Fourth Huntsville Symposium, ed. C. Meegan, R. Preece, & T. Koshut (AIP: New York), 625